

#### Contents lists available at ScienceDirect

#### Fuel

journal homepage: www.elsevier.com/locate/fuel



# Full Length Article



# Techno-economic assessment of modified Fischer-Tropsch synthesis process for direct CO<sub>2</sub> conversion into jet fuel

Yide Han<sup>a</sup>, Ariane D.N. Kamkeng<sup>a</sup>, Olajide Otitoju<sup>a</sup>, Yuxing Ding<sup>a,b</sup>, Meihong Wang<sup>a,\*</sup>

- <sup>a</sup> Department of Chemical and Biological Engineering, The University of Sheffield, Sheffield S1 3JD, UK
- b Key Laboratory of Advanced Control and Optimisation for Chemical Processes, Ministry of Education, East China University of Science and Technology, Shanghai 200237, China

#### ARTICLE INFO

#### Keywords: CO<sub>2</sub> utilisation Modified Fischer-Tropsch synthesis Jet fuel Ex-situ water removal Modelling & simulation Techno-economic assessment

#### ABSTRACT

Direct use of CO2 through modified Fischer-Tropsch synthesis (FTS) process presents a viable approach for the production of carbon-neutral jet fuel. However, achieving high performance for the CO<sub>2</sub>-FTS process remains a significant challenge. Current technology can only achieve low CO2 conversion and low jet fuel yield using tailored catalysts, which hinders the commercial deployment of direct CO<sub>2</sub>-FTS process. This paper presents a techno-economic assessment (TEA) of jet fuel production via CO2-FTS process at commercial-scale. Two ex-situ water removal configurations: (a) multi-stage CO<sub>2</sub>-FTS process and (b) CO<sub>2</sub>-FTS with tail gas recycle process were conducted to assess their potential for performance improvement. Process performance was evaluated using a model developed in Aspen Plus® linking with Aspen Custom Modeller® (ACM), while economic evaluation was carried out in Aspen Process Economic Analyzer®. The CO2-FTS model was based on first principles and modified Anderson-Schulz-Flory (ASF) distribution. Results indicated that both ex-situ water removal configurations can significantly improve the process performance. CO2-FTS process with 90% tail gas recycle has the best performance for both technical and economic analysis. The process achieved 85.8% CO2 conversion and 35.6% jet fuel yield with the lowest energy demand of 4.57 MWh per tonne of produced jet fuel. Moreover, it boasts the lowest minimum selling price (MSP) of jet fuel at US\$2.6/kg despite incurring the second-highest capital expenditure cost of M\$ 451.3. A comparison of the two ex-situ water removal configurations at 61.9% and 76.5% CO2 conversion, suggests that both processes exhibit comparable technical performances, yet the recycling of tail gas holds the potential to reduce economic costs. Consequently, this study will inspire researchers on process improvement and cost reduction of the commercial-scale CO2-FTS jet fuel production.

#### 1. Introduction

#### 1.1. Background

The increasing amount of greenhouse gas (GHG) emissions has led to a global mean temperature rise of more than 1.2  $^{\circ}$ C since the preindustrial era [1]. The International Energy Agency (IEA) has established the target of achieving net-zero CO<sub>2</sub> emissions by roughly midcentury so as to monitor and address the current situation [2]. Among the most difficult emissions to avoid will be those from aviation sector where energy-dense liquid fuels are required and commercially competitive substitutes are lacking [3]. According to the IEA, aviation accounted for 1.03 GtCO<sub>2</sub> (3.1 % total global CO<sub>2</sub> emissions from fossil fuel combustion) in 2019 and this value is projected to reach 1.9 GtCO<sub>2</sub>

in 2050 [4]. Moreover, the jet fuel demand ran at 8 million barrels per day (Mbpd) in 2019 and could rise to 18 Mbpd by 2050 [5]. Therefore, developing technologies to produce sustainable aviation fuels (SAFs) (such as biofuels and synthetic fuels) is needed for decarbonising aviation [6].

 $\mathrm{CO}_2$  conversion can be regarded as a promising approach to produce carbon–neutral products and create a circular economy [7]. A broad range of  $\mathrm{CO}_2$ -derived products, including synthetic fuels (e.g. gasoline and jet fuel) [8–10], chemical materials (e.g. plastics and fibers) [11,12], and building materials (e.g. cement and construction aggregates)[13,14] have been introduced in the literature.  $\mathrm{CO}_2$ -derived fuels can serve as alternatives for hard-to-electrify transportation sectors, including heavy-duty trucks, shipping, and aviation. As these modes of transportation continue to rely partially on liquid fuels, the necessity for new pathways to produce low-carbon synthetic liquid fuels will persist

E-mail address: meihong.wang@sheffield.ac.uk (M. Wang).

<sup>\*</sup> Corresponding author.

bCarbon number at break point $c$ Abbreviations $c$ Olefin desorption rate constant $f_1andf_2$ ACC Fractions of hydrocarbons $k_1, k_5 andk_{6,0}$ Annual capital cost ACM Aspen Custom Modeller® $k_1, k_5 andk_{6,0}$ Kinetic constantsAPEA Aspen Process Economic Analyser $\overline{M}$ Average molecular weight $M_n$ ASF Anderson-Schulz-Flory $M_n$ Molecular weight of hydrocarbon n $N_{HC}$ CAPEX Total molar flowrate of produced hydrocarbons (kmol/hr) $n_i$ CAPEX FTSCapital expenditures FTS $n_{HC_n}$ Molar flowrate of produced hydrocarbons (kmol/hr) $n_i$ FTS HC HydrocarbonFischer-Tropsch synthesis GHG Greenhouse gas $n_i$ Molar flowrate of reactant i (kmol/hr)HC Hydrocarbon $p_i$ Partial pressure (MPa)HC Hydrocarbon $S_n$ Selectivity of hydrocarbon n $W_n$ Mbpd Million barrels per day $S_n$ Selectivity of hydrocarbon n $W_n$ MSP Minimum selling price $V_n$ Weight fraction of hydrocarbon n $V_n$ OPEX Operational expenditures RWGS Reverse water gas shift SAFs Sustainable aviation fuels SOEC Solid oxide electrolysis cell $V_{Jetfuel}$ Yield of jet fuel (mol%) SOEC Solid oxide electrolysis cell	Nomeno	clature	λ	Fitting parameter
α Chain growth probabilities	$c$ $f_1$ and $f_2$ $k_1$ , $k_5$ and $\overline{M}$ $M_n$ $N_{HC}$ $n_{HC_n}$ $n_i$ $P_i$ $S_n$ $W_n$ $X_i$ $X_n$ $Y_{Jetfuel}$ Greek let	Olefin desorption rate constant Fractions of hydrocarbons  dk <sub>6,0</sub> Kinetic constants  Average molecular weight  Molecular weight of hydrocarbon n  Total molar flowrate of produced hydrocarbons (kmol/hr)  Molar flowrate of hydrocarbon n (kmol/hr)  Molar flowrate of reactant i (kmol/hr)  Partial pressure (MPa)  Selectivity of hydrocarbon n  Weight fraction of hydrocarbon n  Conversion of reactant i (mol%)  Mole fraction of hydrocarbon n  Yield of jet fuel (mol%)	ACC ACM APEA ASF CAPEX FTS GHG HC IEA Mbpd MSP OPEX RWGS SAFS SOEC	Annual capital cost Aspen Custom Modeller® Aspen Process Economic Analyser Anderson-Schulz-Flory Capital expenditures Fischer-Tropsch synthesis Greenhouse gas Hydrocarbon International Energy Agency Million barrels per day Minimum selling price Operational expenditures Reverse water gas shift Sustainable aviation fuels Solid oxide electrolysis cell

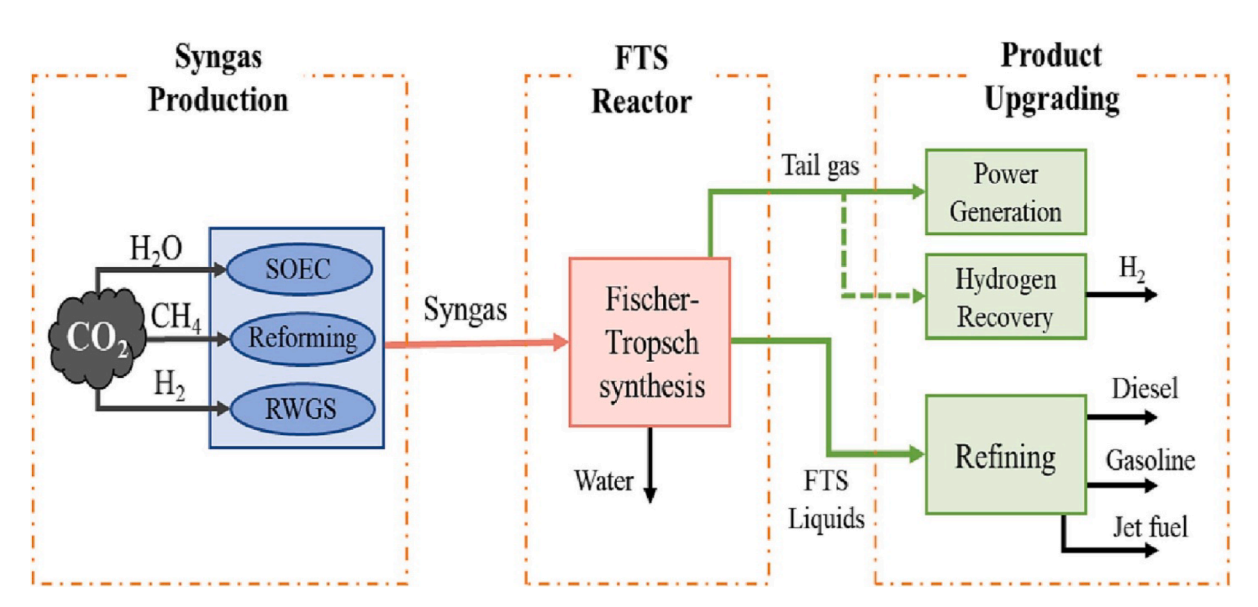


Fig. 1. Block flow diagram of a typical FTS plant [16].

Table 1 Summary of studies performed for CO<sub>2</sub>-FTS process to jet fuel at lab-scale.

Catalyst	Operating pressure (bar)	Operating temperature (°C)	H <sub>2</sub> /CO <sub>2</sub> (mol/ mol)	CO <sub>2</sub> conversion (%)	Jet fuel ( $C_8$ – $C_{16}$ ) selectivity in HC (%)	Jet fuel (C <sub>8</sub> –C <sub>16</sub> ) yield (%)	Ref.
CoFe- 0.81Na	30	240	3	10.2	63.5	6.5	[18]
Fe-Cu	10	300	3	16.7	~37	6.2	[19]
Fe-Zn	10	340	3	34	~49	16.7	[20]
FeK/Co-NC	25	300	3	54.6	~30	16.4	[21]
Fe-Mn-K	10	300	3	38.2	47.8	18.3	[22]

#### [15].

 ${\rm CO_2}$  utilisation via Fischer-Tropsch synthesis (FTS) process provides the pathway to generate synthetic jet fuel. FTS process refers to as a polymerization process which uses syngas (CO and  ${\rm H_2}$ ) as source for the synthesis of hydrocarbon (HC) chains. Reactions (1) to (3) are possible FTS reactions to produce alkanes, olefines and alcohols products. In the indirect method (Fig. 1), there is first syngas production from  ${\rm CO_2}$ 

through oxide electrolysis cell (SOEC), reforming and reverse water gas shift (RWGS) followed by the FTS process in two or more reactors [16]. The one-step method, also known as the modified  $\rm CO_2$ -FTS process has recently gained more attention as it allows the RWGS reaction (4) and FTS reactions (1) to (3) in a single reactor [17].

$$nCO + (2n+1)H_2 \rightarrow C_nH_{2n+2} + nH_2O$$
 (1)

**Table 2**Previous studies on modelling and simulation of CO<sub>2</sub>-FTS process to liquid fuels.

Targeted liquid fuel carbon ranges	Model	Software for model development	Assessment	Ref.
C <sub>5</sub> +	Kinetic model of CO <sub>2</sub> -FTS	CHEMCAD	Process analysis	[23]
FT fuel (carbon ranges NA)	Chemical equilibrium model	Aspen Plus®	TEA	[24]
Gasoline (carbon ranges NA)	Thermodynamic model	Aspen HYSYS®	Economic and environmental assessment	[25]
Gasoline (C <sub>5</sub> –C <sub>11</sub> )	Steady-state CO <sub>2</sub> - FTS model based on a modified ASF distribution	Aspen Plus® using Fortran® Routines	Technical analysis	[16]
Kerosene cut ( $C_{10}$ $-C_{14}$ )	Kinetic model of CO <sub>2</sub> -FTS	Aspen Plus®	TEA	[26]
e-kerosene (carbon ranges NA)	Chemical equilibrium model	Aspen Plus®	Process analysis	[27]

**Table 3** Products and chemical reactions implemented for CO<sub>2</sub>-FTS model.

Carbon range	Product category	Carbon number	Component	Chemical reaction
n = 1	CO Methane	1	CO CH <sub>4</sub>	$CO_2 + H_2 \rightarrow CO + H_2O$ $CO + 3H_2 \rightarrow CH_4 +$ $H_2O$
$2 \le n \le 4$	Light HCs (C <sub>2</sub> –C <sub>4</sub> )	2, 3 and 4	$C_2H_6$	$2CO + 5H_2 \rightarrow C_2H_6 + 2H_2O$
	(02 04)		$C_2H_4$	$2CO + 4H_2 \rightarrow C_2H_4 + 2H_2O$
			$C_3H_8$	3CO + 7H <sub>2</sub> →C <sub>3</sub> H <sub>8</sub> + 3H <sub>2</sub> O
			$C_3H_6$	3CO + 6H <sub>2</sub> →C <sub>3</sub> H <sub>6</sub> + 3H <sub>2</sub> O
			$C_4H_{10}$	$4CO + 9H_2 \rightarrow C_4H_{10} + 4H_2O$
			$C_4H_8$	4CO + 8H <sub>2</sub> →C <sub>4</sub> H <sub>8</sub> + 4H <sub>2</sub> O
$5 \le n \le 7$	C <sub>5</sub> –C <sub>7</sub> HCs	5, 6 and 7	$C_5H_{12}$	5CO + 11H <sub>2</sub> →C <sub>5</sub> H <sub>12</sub> + 5H <sub>2</sub> O
			$C_5H_{10}$	$5CO + 10H_2 \rightarrow C_5H_{10} + 5H_2O$
			$C_6H_{14}$	$6CO + 13H_2 \rightarrow C_6H_{14} + 6H_2O$
			$C_6H_{12}$	$6CO + 12H_2 \rightarrow C_6H_{12} + 6H_2O$
			$C_7H_{16}$	$7CO + 15H_2 \rightarrow C_7H_{16} + 7H_2O$
			$C_7H_{14}$	$7CO + 14H_2 \rightarrow C_7H_{14} + 7H_2O$
$8 \le n \le 16$	Jet Fuel (C <sub>8</sub> –C <sub>16</sub> )	12	$C_{12}H_{26}$	$12CO + 25H_2 \rightarrow C_{12}H_{26} +$
			$C_{12}H_{24}$	$\begin{array}{l} 12H_{2}O \\ 12CO + \\ 24H_{2} \! \rightarrow \! C_{12}H_{24} + \end{array}$
$n \ge 17$	Wax	20	$C_{20}H_{42}$	$\begin{array}{c} 12 H_{2} O \\ 20 CO + \\ 41 H_{2} \rightarrow C_{20} H_{42} + \\ 20 H_{2} O \end{array}$

$$nCO + 2nH_2 \rightarrow C_nH_{2n} + nH_2O \tag{2}$$

$$nCO + 2nH_2 \rightarrow C_nH_{2n+1}OH + (n-1)H_2O$$
 (3)

$$CO_2 + H_2 \rightleftharpoons CO + H_2O \tag{4}$$

#### 1.2. Literature review

The products from the modified  $CO_2$ -FTS process can be wide since a variety of catalysts can be used. This paper (hence, the literature review) focuses on the synthesis of jet fuel from  $CO_2$ -FTS process. To date, the modified  $CO_2$ -FTS process for  $CO_2$  conversion into jet fuel has only been reported at laboratory scale. A summary of a few studies on the  $CO_2$ -FTS process to jet fuel ( $C_8$ - $C_{16}$ ) is presented in Table 1. Most studies reported Fe and Co-based catalysts and achieved up to 64 % selectivity to jet fuel whereas,  $CO_2$  conversion varies from 10 % to 55 % [18–22]. The largest jet fuel yield of 18.3 % can be found from Yao et al. [22].

Table 2 presents an overview of previous studies on modelling and simulation for the modified CO<sub>2</sub>-FTS process to liquid fuels. Meier et al. [23] developed a kinetic model comprising 20 reactions to study CO<sub>2</sub>-FTS plant performance through periodical removal of water for C<sub>5</sub><sup>+</sup> hydrocarbons. The authors looked into ex-situ water removal to improve CO<sub>2</sub>-FTS reaction rates and C<sub>5</sub> + selectivity. Zang et al. [24] assessed the synthesis of liquid fuels (C5+) through a techno-economic assessment (TEA) of the CO<sub>2</sub>-FTS process and predicted the minimum selling price (MSP) of the FT fuel is \$5.4-5.9/gal (throughout this paper, \$ always refers to USD). Fernandez-Torres et al. [25] applied Aspen-HYSYS® to design and optimise CO2-FTS to gasoline at commercial-scale. For a gasoline production rate of 23.65 ton/hr, their results indicated that the capital expenditures (CAPEX) and operational expenditures (OPEX) are in the ranges of 73 to 128 M\$ and 244 to 1951 M\$/yr, respectively. Kamkeng and Wang [16] studied the performance improvement of the CO<sub>2</sub>-FTS process for gasoline (C<sub>5</sub>-C<sub>11</sub>) production using ex-situ water removal. The authors developed a CO<sub>2</sub>-FTS model based on first principles and a modified Anderson-Schulz-Flory (ASF) distribution, which was implemented in Aspen Plus® using Fortran® Routines and validated with laboratory data. The results demonstrated that the use of ex-situ water removal technique can increase CO2 conversion and gasoline yield by up to 34 % and 70 %, respectively. The single CO<sub>2</sub>-FTS reactor with recycle and three-stage CO<sub>2</sub>-FTS reactors in series showed a similar process efficiency of 66.4 %. However, economic analysis was not evaluated to indicate the feasibility of commercial deployment. Colelli et al. [26] carried out the comparative TEA for the indirect and direct production of synthetic kerosene ( $C_{10}-C_{14}$ ) via FTS. They predicted the productivity of the plant (66.18 bbl/d and 38.46 bbl/d) and product cost (460 to 1435 €/bbl and 752 to 2364 €/bbl) for the indirect and direct process. However, their simulation results based on kinetic model present very large relative errors (-38.6-77.8 %) compared with experimental data. Atsonios et al. [27] investigated four different thermochemical pathways for CO2 conversion into synthetic kerosene using chemical equilibrium models developed in Aspen Plus®. They indicated that the low-temperature CO conversion through RWGS and FTS is the most energy efficient pathway, but the economic evaluation is not included for comparison.

#### 1.3. Aim and novel contributions of this paper

In this study, a TEA was carried out for direct  $CO_2$  conversion into jet fuel ( $C_8$ – $C_{16}$ ) via  $CO_2$ -FTS process at commercial scale. Two ex-situ water removal configurations were considered for jet fuel yield improvement. This study provides the following novel contributions:

(1) This study proposes an advanced model based on first principles and a modified ASF for jet fuel production from CO<sub>2</sub>-FTS process. The CO<sub>2</sub>-FTS model was implemented in Aspen Plus® linking

Fig. 2. Flowsheet diagram of CO<sub>2</sub>-FTS process implemented in Aspen Plus® using Fortran® Routines.

**Table 4**Input parameters used for model validation.

Parameter		Value	Reference
Reactor type		fixed bed	[22]
Reactor diameter (cm)		1	
Reactor temperature (°C)		300	
Reactor pressure (MPa)		1	
H <sub>2</sub> /CO <sub>2</sub> ratio		3	
Flow rate (mL/min)		40	
CO <sub>2</sub> conversion (%)		38.2	
Chain growth probability	$\alpha_1$	0.79	500.001
	$\alpha_2$	0.57	[22,29]
Carbon number at breakpoint		12	
Kinetic constants	$\mathbf{k_1}$	$1.66 \times 10^{-2}$	
	k <sub>5</sub>	$6.99 \times 10^{-5}$	[16,30]
	K <sub>6.0</sub>	$2.02\times10^{\text{-}2}$	
Constant c		-0.26	
Fitting parameter $\lambda$	$n \le 7$	$0.15e^{0.35n}$	
	$8 \le n \le 12$	$0.29e^{0.39n}$	
	$n \ge 13$	$2.7e^{36n^{-1}}$	

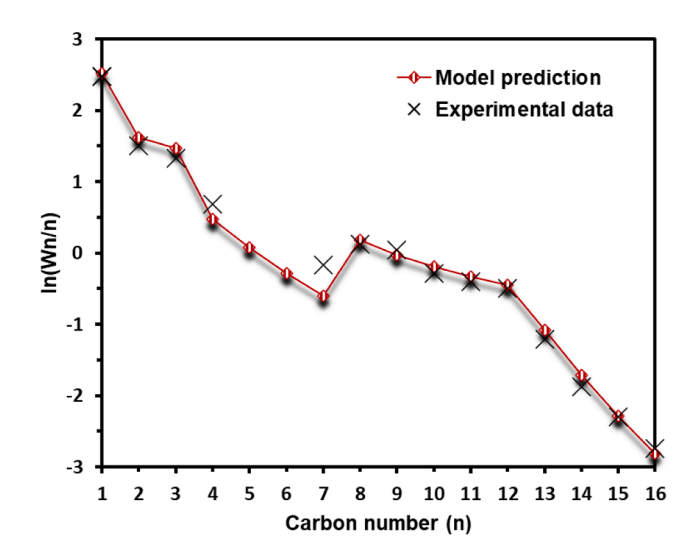


Fig. 3. Model prediction of ASF plot compared with experimental data.

with Aspen Custom Modeller® (ACM) and validated using experimental data [22].

(2) Although ex-situ water removal has been previously considered for CO<sub>2</sub>-FTS process improvement [16,23], this technique has never been applied for CO<sub>2</sub>-FTS to jet fuel. Therefore, this study looks into two ex-situ water removal configurations (reactors in series and a single reactor with recycle) assess its potential in performance improvement during jet fuel production through the CO<sub>2</sub>-FTS process.

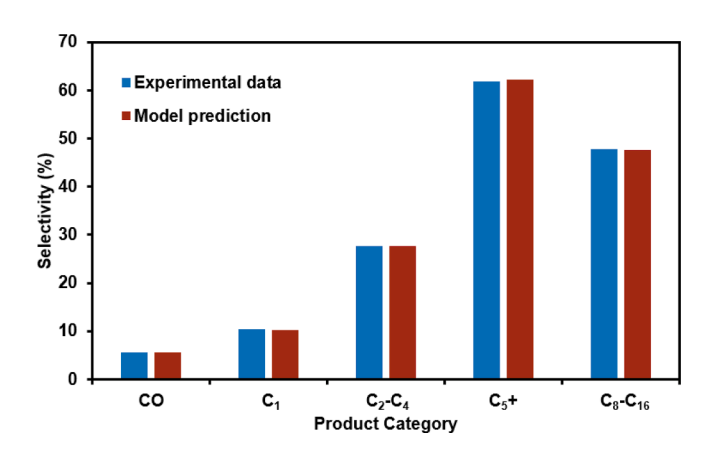


Fig. 4. Model prediction and experimental values of  $CO_2$ -FTS product selectivity.

**Table 5**Model validation results of selectivity for different product category.

Product category	Selectivity (%) Experimental data	Model prediction	Relative error (%)
CO	5.6	5.60	0.00
$C_1$	10.4	10.14	-2.51
C2-C4	27.7	27.60	0.34
$C_{5+}$	61.9	62.26	0.58
C <sub>8</sub> -C <sub>16</sub>	47.8	47.64	-0.34

(3) A comparative TEA is carried out for the two ex-situ water removal configurations of the CO<sub>2</sub>-FTS process. This analysis aims to provide with relevant information to decision-makers on the commercial application of jet fuel produced from CO<sub>2</sub>-FTS process.

### 2. Model development and validation of CO<sub>2</sub>-FTS process

# 2.1. Model development

#### 2.1.1. Assumptions

The following assumptions were made during  ${\rm CO}_2{\text{-FTS}}$  model development:

- CO<sub>2</sub>-FTS process operates at steady-state condition. Hence, the accumulation of heat and mass was not considered.
- Only reactant conversion and specific products are considered based on material balance and stoichiometric reactions.
- The type of HCs depends on the nature of catalyst. Since the selectivity towards oxygenated compounds was below 1.0 % during experiments [22], they were neglected in this model. Hence, only olefins and paraffins were considered in this model.

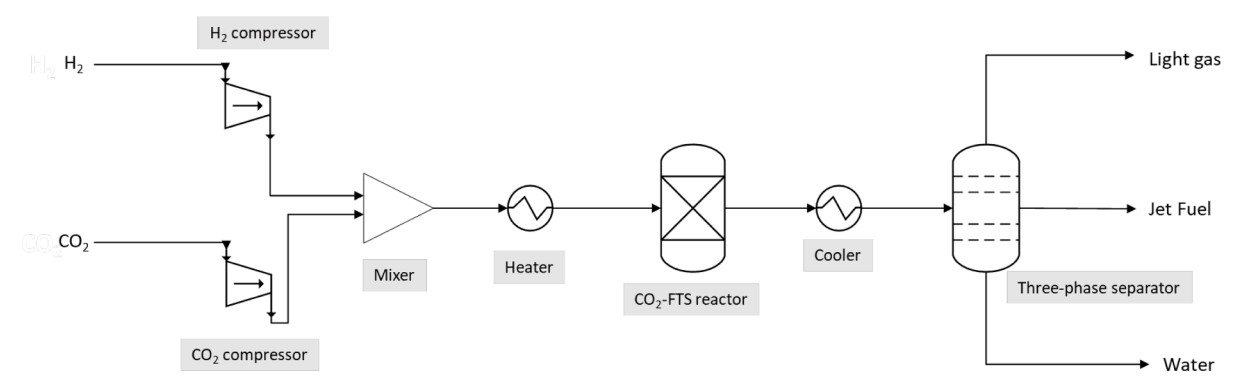


Fig. 5. Base case scenario of the CO<sub>2</sub>-FTS plant for jet fuel production.

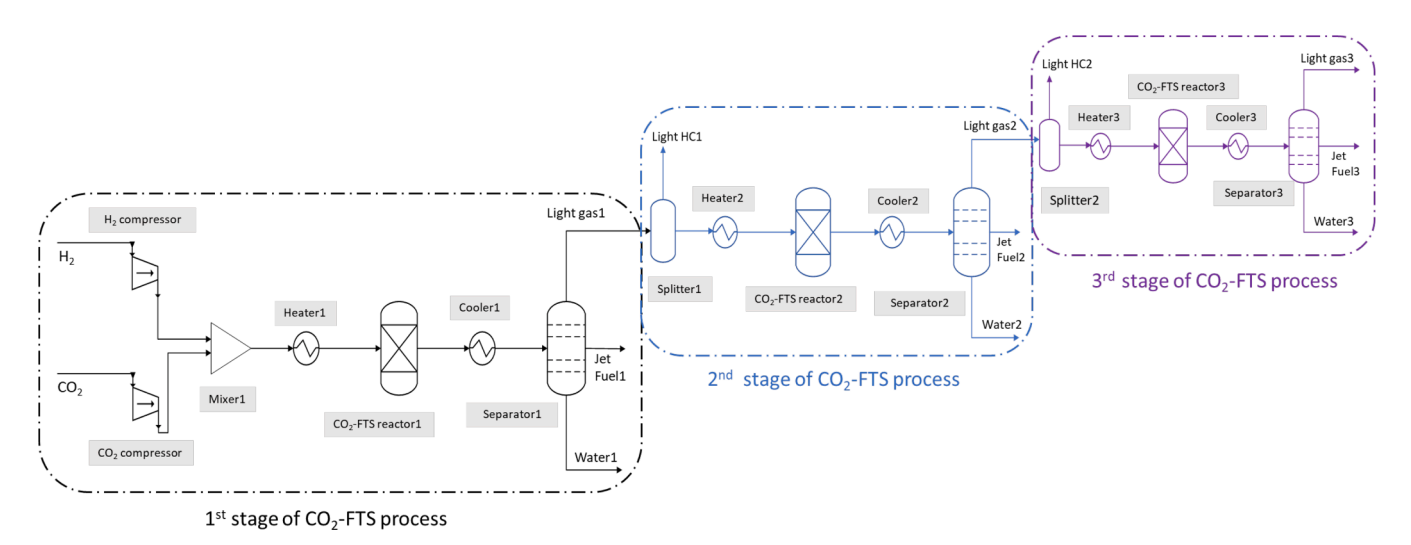


Fig. 6. Multi-stage  $CO_2$ -FTS plant for jet fuel production.

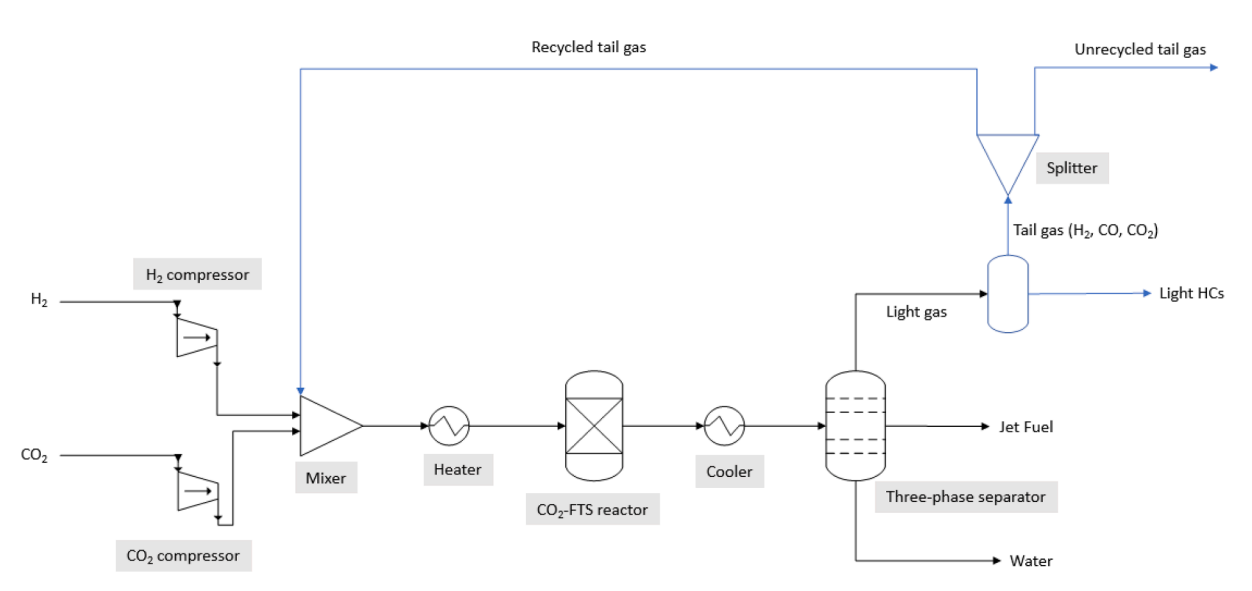


Fig. 7. CO<sub>2</sub>-FTS with tail gas recycle plant for jet fuel production.

- The chain growth probability of hydrocarbons was based on given Anderson-Schulz-Flory (ASF) plot from experiments [22].
- The large number of CO<sub>2</sub>-FTS reactions was handled by lumping technique. It is simply defined as grouping several components into a smaller number of components to represent the whole group [28].

# 2.1.2. Modelling of hydrocarbon distribution

A model for the prediction of hydrocarbon distribution was developed in ACM. This model combines modified ASF theory and kinetic modelling of  $CO_2$ -FTS process to accurately predict the hydrocarbon distributions. Based on the previous modified ASF model, the weight fraction of hydrocarbon  $(W_n)$  was calculated from Eq. (5) [29] based on

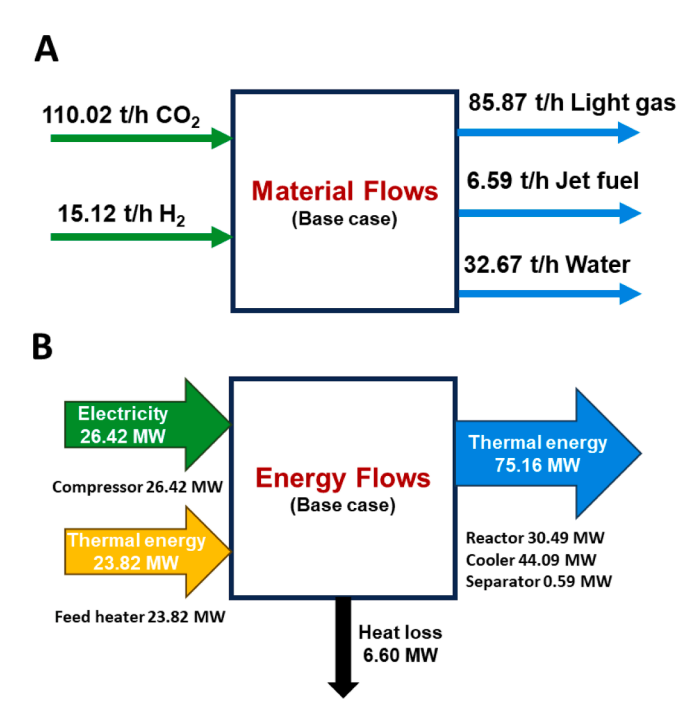


Fig. 8. Material and energy flows of base case.

**Table 6**Performance summary of the base case CO<sub>2</sub>-FTS process.

Parameter		Value
Jet fuel features	Mass flowrate (tonne/h)	6.59
	Density at 15 °C (kg/m <sup>3</sup> )	741.89
	Viscosity at −20 °C (mm <sup>2</sup> /s)	2.70
	Flash point (°C)	77.37
Energy consumption (MW)	Compressors	26.42
	Feed heater	23.82
	Reactor cooling jackets	30.49
	Syncrude coolers	44.09
	Flash drums	0.59
	Heat losses	6.60
Energy input (MW)		50.24
Total energy consumption (M	W)	132.00
Energy consumption for each	tonne captured CO2 (kWh/t-CO2)	456.67
Energy consumption for each	tonne produced jet fuel (MW/t-Jet fuel)	7.62
CO <sub>2</sub> conversion (mol%)		38.20
Jet fuel yield (mol%)		17.18

two chain growth probabilities ( $\alpha_1$  and  $\alpha_2$ ) and two fractions of hydrocarbons ( $f_1$  and  $f_2$ ).

$$W_n = f_1 \times \alpha_1^{n-1} + f_2 \times \alpha_2^{n-1}$$
 (5)

The  $C_3$  hydrocarbon is considered a deviation from the standard ASF distribution due to the complex reaction mechanisms of the Fe-Mn-K catalyst used. Consequently, specific experimental conditions and kinetic values were employed to accurately model the chain growth probability and weight fraction for  $C_3$  hydrocarbons. The chain growth probability of  $C_3$  ( $\alpha_{C_3}$ ), as shown in Eq. (6), was calculated using the specific experimental conditions ( $P_{CO_2}$  and  $P_{H_2}$ ) and kinetic values ( $k_1$ ,  $k_5$  and  $k_{6,0}$ ) suggested by Kamkeng and Wang [16].

$$\alpha_{C_3} = \frac{k_1 P_{CO_2}}{k_1 P_{CO_2} + k_5 P_{H_2} + k_{6,0} e^{3c}}$$
 (6)

The weight fraction of  $C_3$  compounds ( $W_3$ ) can be calculated from Eq. (7) using chain growth probability of  $C_3$ .

$$W_3 = 3 \times (1 - \alpha_{C_3})^2 \times \alpha_{C_3}^2 \tag{7}$$

Two fractions of hydrocarbons ( $f_1$  and  $f_2$ ) related to  $\alpha_1$  and  $\alpha_2$  are derived from Eqs. (8) and (9) based on carbon number at break point (b) and fitting parameter ( $\lambda$ ).

$$f_{1} = \lambda \frac{1 - W_{3}}{\frac{1}{1 - \alpha_{1}} - \frac{\alpha_{1}}{1 + \alpha_{1}} + \left[ \frac{1}{1 - \alpha_{2}} - \frac{\alpha_{2}}{1 + \alpha_{2}} \right] \left( \frac{\alpha_{1}}{\alpha_{2}} \right)^{b-1}}$$
(8)

$$f_2 = f_1 \times \left(\frac{\alpha_1}{\alpha_2}\right)^{b-1} \tag{9}$$

The mass fraction of hydrocarbons obtained from ASF theory is converted into corresponding selectivity  $(S_n)$  by applying Eqs. (10)–(12).

$$\frac{1}{\overline{M}} = \sum_{n=1}^{50} \frac{W_n}{M_n} \tag{10}$$

$$x_n = \frac{W_n}{M_-} \times \overline{M} \tag{11}$$

$$S_n = \frac{x_n \times n}{\sum_{n=1}^{50} x_n \times n} \tag{12}$$

where  $M_n$  is the molecular weight of hydrocarbon n,  $\overline{M}$  is the average molecular weight, and  $x_n$  is the mole fraction of hydrocarbon.

With the obtained selectivity of hydrocarbons, the molar flowrate for each carbon compounds  $(n_{HC_n})$  are calculated based on Eqs. (13) and (14).

$$N_{HC} = n_{CO_{2in}} \times X_{CO_2} \times X_{CO} \tag{13}$$

$$n_{HC_n} = N_{HC} \times \frac{S_n}{n} \tag{14}$$

where  $N_{HC}$  is the total molar flowrate of produced hydrocarbons,  $X_i$  is the conversion of reactant i, and  $n_i$  is molar flowrate of reactant i.

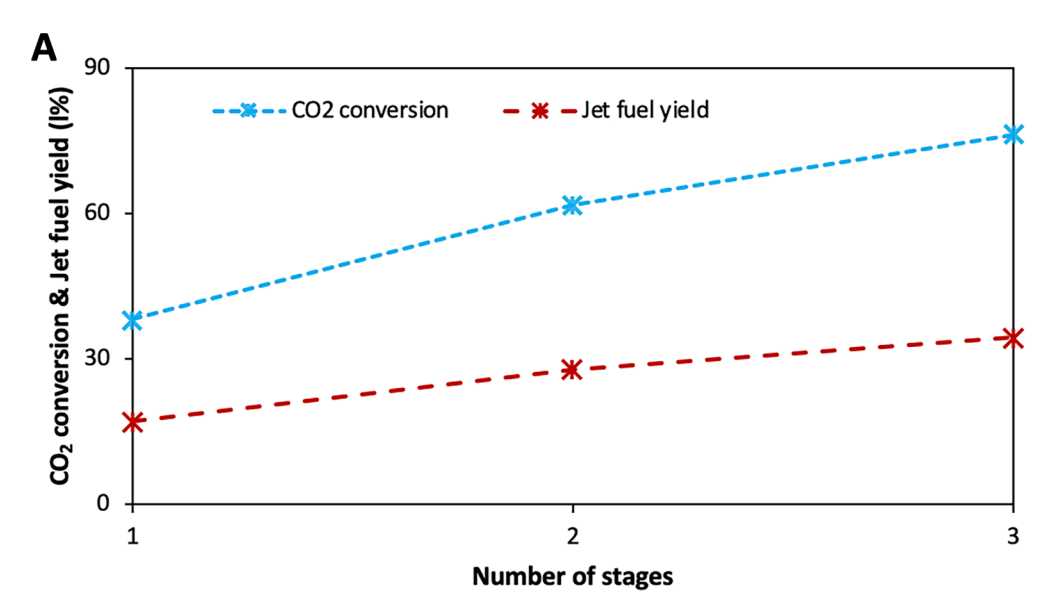
# 2.1.3. Model implementation of CO<sub>2</sub>-FTS process using Aspen Plus® linking with Aspen customer modeller®

The CO<sub>2</sub>-FTS process was implemented in Aspen Plus® linking with ACM. Initially, the modified ASF distribution model was calculated in ACM® for every carbon number ranging from 1 to 50. The CO<sub>2</sub>-FTS reactions and lumping components used for process modelling are presented in Table 3. For simplicity, the wax category represents hydrocarbons with carbon numbers greater than 17, encompassing both waxes and any minimal higher-carbon components such as diesel. Based on the olefin to paraffin ratio specified in the experimental study, the flowrate of the corresponding carbon number can determine each product.

Fig. 2 illustrates the CO $_2$ -FTS process flowsheet implemented in Aspen Plus® using the physical property method Peng-Robinson. The ACM model was exported as a calculation block (FLOWRATE) to Aspen Plus® flowsheet for calculating the flowrate of hydrocarbons presented in Table 3. With the help of Fortran® Routines, the PRODUCT stream is correlated to ACM model. The feedstock  $H_2$  and  $CO_2$  were assumed to be at 25 °C and 1 bar. They are first compressed at 10 bar with a 2-stage compressor featuring intercooling. Afterwards, they were mixed and heated at 300 °C in a heater (HEATER). The  $CO_2$ -FTS reactor which performs the RWGS and FTS reactions is represented by a stoichiometry reactor block ( $CO_2$ -FTS) in Aspen Plus®.

#### 2.2. Model validation

To validate the developed CO<sub>2</sub>-FTS model, lab-scale experiments conducted at the University of Oxford were used. The experiments provide ASF plots and selectivity for different carbon categories for model validation. The ratio of olefin to paraffin for each hydrocarbon is obtained from experiments [18,22]. The input process conditions and



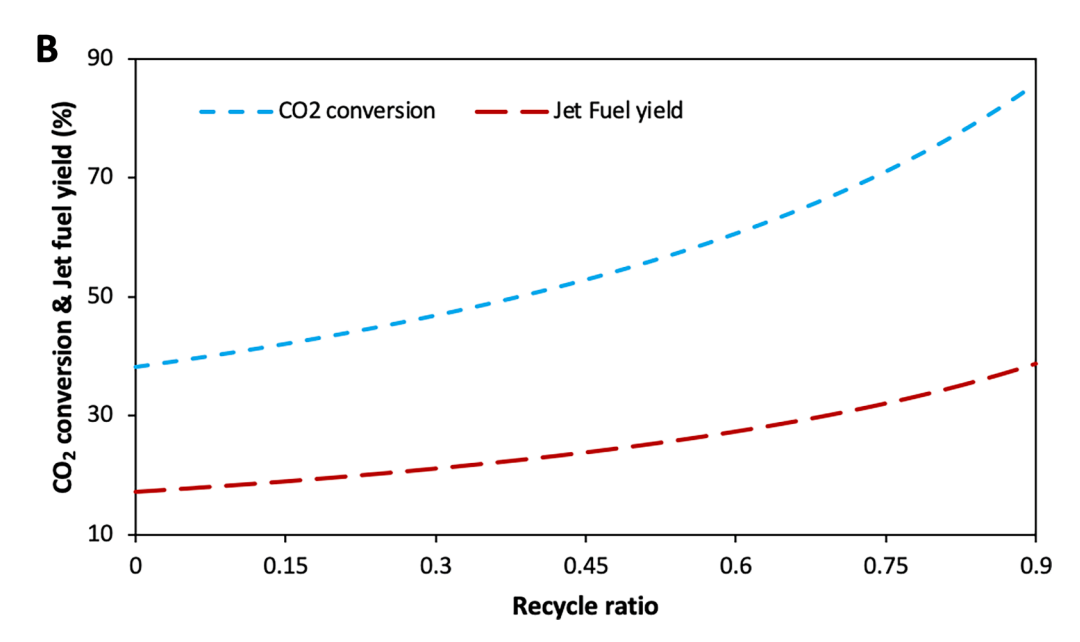


Fig. 9. Performance prediction of CO<sub>2</sub> conversion and jet fuel yield for CO<sub>2</sub>-FTS process under two ex-situ water removal configurations: (A) Multi-stage CO<sub>2</sub>-FTS process, and (B) CO<sub>2</sub>-FTS with tail gas recycle.

parameters used for the CO<sub>2</sub>-FTS model validation are presented in Table 4. Process conditions were available from Yao et al. [22], other parameters were reasonably assumed based on literature.

Fig. 3 compares the model prediction results of the ASF plots with the experimental data given from carbon numbers 1 to 16. The ASF plots agree with the experimental trend and model values. On the other hand, Fig. 4 compared five product categories of model prediction results with experimental data. All the relative errors shown in Table 5 are below 2.5 %. Therefore, Figs. 3 and 4 show great agreement of the developed model with experimental work.

# 3. Simulation of the modified $CO_2$ -FTS process for jet fuel production at commercial scale

#### 3.1. Base case scenario

The base case scenario is the  $CO_2$ -FTS process using a single reactor. The process features an open-loop configuration without the

recirculation or upgrade of unconverted reactants, water removal and/or reactor design. The results obtained from the base case scenario were used as a reference for performance comparison between the optimised plants.

The process flow diagram of the base case scenario developed in Aspen Plus® linking with ACM is shown in Fig. 5. The inlet flowrate of  $\rm CO_2$  and  $\rm H_2$  were chosen 110.02 t/h and 15.12 t/h, respectively. This was based on commercial  $\rm CO_2$  utilisation plant in previous studies [16,25]. In the base case scenario, the products leaving the reactor are cooled down to 40 °C according to industry operation for syncrude oil separation. Finally, a three-phase separator divides the stream into light gas, jet fuel and water.

### 3.2. Ex-situ water removal configurations for CO<sub>2</sub>-FTS process

Previous studies (both experimental and modelling) have demonstrated that water formation during  $CO_2$ -FTS process significantly inhibits  $CO_2$  conversion due to a decrease in the driving force of the RWGS

**Table 7**Performance summary of the multi-stage CO<sub>2</sub>-FTS process.

Parameter		Two- stage	Three- stage
Jet fuel features	Mass flowrate (tonne/h)	11.07	13.86
	Density at 15 °C (kg/m <sup>3</sup> )	741.55	741.31
	Viscosity at −20 °C (mm <sup>2</sup> /s)	2.67	2.65
	Flash point (°C)	77.36	77.35
Energy consumption	Compressors	26.42	26.42
(MW)	Feed heater	38.41	47.05
	Reactor cooling jackets	51.59	64.75
	Syncrude coolers	71.82	88.62
	Flash drums	0.98	1.23
	Heat losses	9.96	12.00
Energy input (MW)		64.83	73.47
Total energy consumption	on (MW)	199.19	240.07
Energy consumption for t-CO <sub>2</sub> )	each tonne captured CO <sub>2</sub> (kWh/	589.25	667.78
Energy consumption for (MW/t-Jet fuel)	each tonne produced jet fuel	5.86	5.30
CO <sub>2</sub> conversion (mol %)	1	61.86	76.46
Jet fuel yield (mol %)		27.82	34.38

**Table 8** Performance summary of CO<sub>2</sub>-FTS with tail gas recycle process.

Parameter		63.8 % recycle	80.3 % recycle	90 % recycle
Jet fuel	Mass flowrate (tonne/h)	11.33	13.83	15.94
features	Density at 15 °C (kg/m <sup>3</sup> )	741.32	740.75	739.41
	Viscosity at −20 °C (mm <sup>2</sup> /s)	2.65	2.60	2.48
	Flash point (°C)	77.36	76.91	69.00
Energy	Compressor	26.42	26.42	26.42
consumption	Pre-heater	23.82	38.47	44.61
(MW)	Reactor cooling jackets	52.78	64.28	73.46
	Syncrude coolers	72.62	85.94	93.67
	Flash drums	1.01	1.23	1.41
	Heat losses	10.07	11.71	12.71
Energy input (MV	N)	64.90	71.03	72.92
Total energy cons	sumption (MW)	201.37	234.19	254.17
Energy consumpt CO <sub>2</sub> (kWh/t-CO	ion for each tonne captured O <sub>2</sub> )	589.85	645.63	662.78
Energy consumpt fuel (MW/t-Jet	ion for each tonne produced jet fuel)	5.73	5.14	4.57
CO <sub>2</sub> conversion (	mol %)	61.86	76.46	85.82
Jet fuel yield (mo	ol %)	27.82	34.38	35.59

reaction. Therefore, continuous water removal is essential to improve RWGS reaction rate hence,  $CO_2$  conversion.

#### 3.2.1. Multi-stage CO2-FTS process

Fig. 6 depicts the concept of a multi-stage  $CO_2$ -FTS process, which is created by connecting continuous stages of  $CO_2$ -FTS process in series. This multi-stage design incorporates multiple  $CO_2$ -FTS reactors by reusing unreacted feedstocks from previous stages. The process was simulated in Aspen Plus® linking with ACM. Although several stages can be interconnected, this paper only investigated two-stage and three-stage for the  $CO_2$ -FTS process.

In a typical three-stage  $\mathrm{CO}_2$ -FTS process, the first stage corresponds the base case scenario aforementioned. The second and third stages employ the same process as the base case but exclude compressors and incorporates additional separators to split light hydrocarbons. For the first stage, the feed stream contains only  $\mathrm{H}_2$  and  $\mathrm{CO}_2$  to the  $\mathrm{CO}_2$ -FTS reactor while for the second and third stages, the feed stream also includes unconverted  $\mathrm{CO}_2$ ,  $\mathrm{H}_2$  and  $\mathrm{CO}$ . The operating conditions for each stage were same as the base case process shown in Table 4.

# 3.2.2. CO<sub>2</sub>-FTS with tail gas recycle process

The ex-situ water removal for CO<sub>2</sub>-FTS process through tail gas recycle (Fig. 7) was also simulated in Aspen Plus® linking with ACM. In

comparison to the base case process, the tail gas (unreacted  $H_2$ , CO, and  $CO_2$ ) is separated from the light gas and recycled to the mixer. The recycled tail gas flowrate depends on the recycle ratio set in the splitter. The splitter separates tail gas with  $H_2$  to  $CO_2$  ratio of 3 to meet the strict operating condition under Fe-Mn-K catalyst. Since only the ratio of 3 is studied in the experiments, the other ratio of the reaction circumstance is unknown. The study of different recycle ratio is carried out by sensitivity analysis in Aspen Plus®. It should be noted that the recycle ratio was initially set from 0 to 100 %. However, only 0–90 % can be realised in Aspen Plus® due to the convergence of software. The recycled tail gas is mixed with the feedstock before preheating in the heater. Unrecycled tail gas and light hydrocarbons is not onsidered for further application.

# 4. Technical analysis of the modified CO<sub>2</sub>-FTS process for jet fuel production at commercial scale

#### 4.1. Assumptions and performance metrics

Process analysis of  $CO_2$ -FTS process was performed under the following assumptions.

- The CO<sub>2</sub>-FTS reactor and Fe-Mn-K catalyst behave the same way at lab-scale and commercial-scale.
- 5 % heat losses were assumed during whole CO<sub>2</sub>-FTS operating units
- No pressure drop was assumed in the heaters and coolers.
- CO<sub>2</sub> conversion ( $X_{CO_2}$ ) and jet fuel yield ( $Y_{Jetfuel}$ ) are calculated based on Eqs. (15) and (16).

$$X_{CO_2} = \frac{nCO_{2_{in}} - nCO_{2_{out}}}{nCO_{2_{in}}}$$
 (15)

$$Y_{Jetfuel} = X_{CO_2} \times S_{Jetfuel} \tag{16}$$

### 4.2. Base case scenario

The results of the material and energy balance of the base case CO<sub>2</sub>-FTS process are shown in Fig. 8. The base case CO<sub>2</sub>-FTS plant leads to roughly 6.59 t/h of jet fuel, 85.87 t/h of light gas and 32.67 t/h of water (Fig. 8A). Fig. 8B shows the total energy input (26.42 MW electricity and 23.82 MW thermal energy) to the system, the energy output from the system (75.16 thermal energy), and the assumed heat loss (6.60 MW). Note that most of the thermal energy output is from cooling energy (30.49 MW reactor cooling jackets and 44.09 MW syncrude cooler). Compared to the previous study by Kamkeng and Wang [16], total energy in this study is reduced by 23.35 MW. This is mainly due to the lower energy consumption in the compressors (26.42 MW compared to 70.79 MW). In fact, for the jet fuel production the operating pressure is only 10 bar which is one third of the gasoline production [16].

The performance summary is presented in Table 6 which shows jet fuel characteristics, energy consumption for each sector, CO2 conversion and jet fuel yield. The direct CO2-FTS process achieves a jet fuel selectivity of 47.6 %, however the jet fuel yield is only 17.2 % due to low CO<sub>2</sub> conversion (38.2 %). Considering the selectivity towards C<sub>17+</sub> hydrocarbons is roughly 2.0 %, for simplicity, the distillation and hydrocracking processes were not considered [16]. The energy consumption for feedstock of CO<sub>2</sub> and the product of jet fuel were calculated and respectively are 456.67 kWh per ton of feedstock CO2 and 7.62 MW per ton of produced jet fuel. The density of jet fuel was found 742 kg/m<sup>3</sup> from the model which is close to the synthetic paraffinic kerosene (749 kg/m<sup>3</sup>) from previous literature [31]. However, these values are lower than the commercial jet fuels Jet A and Jet A-1 (775–840  $kg/m^3$ ) [32]. This could be due to the absence of aromatic compounds in the produced jet fuel. For future commercialisation to reach the standard jet fuel density level, further approaches can be adopted, such as adding appropriate fuel additives and blending with conventional jet fuel [33].



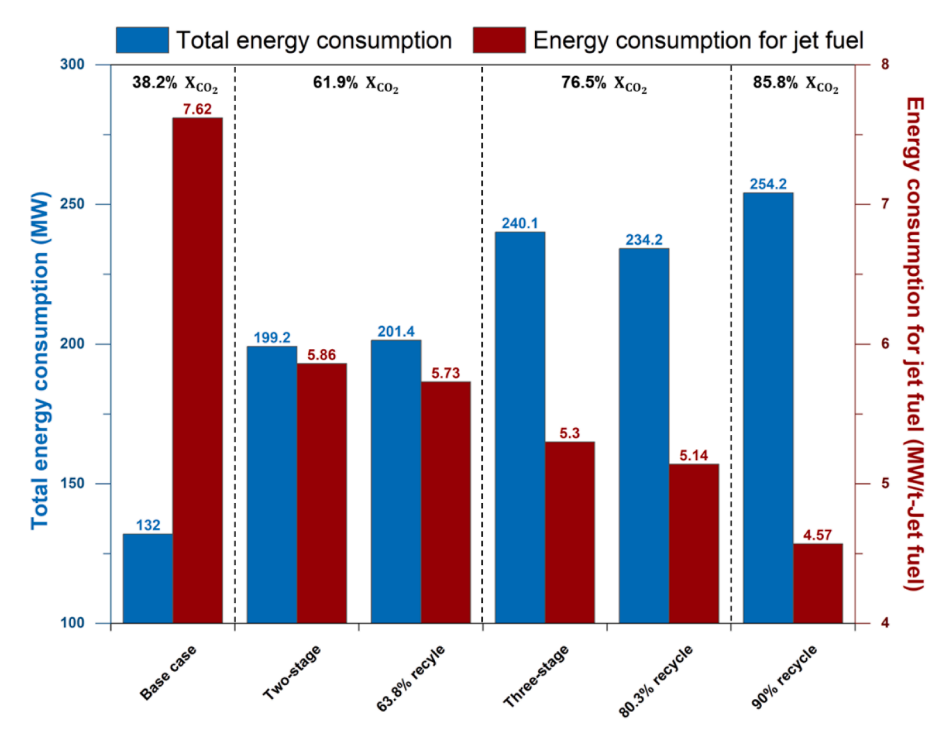


Fig. 10. Summary of energy consumption for different CO<sub>2</sub>-FTS process.

**Table 9** Financial parameters used in economic analysis.

Parameter	Value	Reference
CO <sub>2</sub> price (\$/kg)	0	[35]
H <sub>2</sub> price (\$/kg)	2	[36]
Heating price (\$/GJ)	4.25	[34]
Cooling water utility cost (\$/tonne)	0.35	[34]
Electricity price (\$/kWh)	0.0775	[34]
Operating time per year (hour)	8000	[34]
Plant lifetime (year)	20	[25]
Interest rate (%)	10	[25]

#### 4.3. Performance prediction for the ex-situ water removal configurations

#### 4.3.1. CO<sub>2</sub> conversion and jet fuel yield

Fig. 9 shows the predicted trends of using multi-stage CO<sub>2</sub>-FTS process and CO<sub>2</sub>-FTS with tail gas recycle process. Both ex-situ water removal configurations show improvement in CO<sub>2</sub> conversion and jet fuel yield. With the addition of the number of stages, the CO<sub>2</sub> conversion increases from 38.2 % to 61.9 % at two stages and 76.5 % at three stages. On the other hand, recycling 90 % tail gas achieved 85.8 % CO<sub>2</sub> conversion and 35.6 % jet fuel yield. With the design specification method in Aspen Plus®, two recycle ratio points (63.8 % and 80.3 %) were calculated, corresponding to the same CO<sub>2</sub> conversion in the two-stage and three-stage CO<sub>2</sub>-FTS process. From the standpoint of improving CO<sub>2</sub> conversion and jet fuel yield, adding the number of stages to the CO<sub>2</sub>-FTS process and adopting tail gas recycling have the same function.

#### 4.3.2. Energy consumption

With the improvement in  $\rm CO_2$  conversion and jet fuel yield, the energy consumption also increased for both ex-situ water removal configurations. Tables 7 and 8 present the performance summary for the multi-stage  $\rm CO_2$ -FTS process and  $\rm CO_2$ -FTS with tail gas recycling. The multi-stage  $\rm CO_2$ -FTS process showed 1.7 times increase in jet fuel productivity for the two-stage process and 2.1 times increase for the three-stage process, respectively. The energy demand for compressors remains the same because feedstock is compressed only in the first stage. The

increase in the total energy demand is mainly due to the thermal energy demand in the 2nd and 3rd stages of the  $\rm CO_2$ -FTS process. Although the total energy consumption and the energy consumption per ton of feed-stock  $\rm CO_2$  increase with the addition of stages to the  $\rm CO_2$ -FTS process, the energy consumption per ton of jet fuel produced decreases. The same performance trends were found for the tail gas recycle case. As the recycle rate increases, the total energy demand rises while the energy demand for each ton of jet fuel produced decreases.

#### 4.3.3. Comparison between two ex-situ water removal configurations

To find out the energy consumption between the two ex-situ water removal configurations, they were compared at the same  $CO_2$  conversion (61.9 % and 76.5 %). Therefore, in Fig. 10, the two-stage  $CO_2$ -FTS process is compared to the  $CO_2$ -FTS process with 63.8 % tail gas recycle, and the three-stage  $CO_2$ -FTS process is compared to the  $CO_2$ -FTS process with 80.3 % tail gas recycle. The tail gas recycle process consumed more total energy at 61.9 %  $CO_2$  conversion compared to the multi-stage process, while the result is reversed at 76.5 %  $CO_2$  conversion. In terms of jet fuel energy consumption, the tail gas recycle process requires less energy for  $CO_2$  conversion at 61.9 % and 76.5 % scenarios. Therefore, the economic evaluation should be carried out to provide further guidance.

On the other hand, when these two water removal approaches are compared with the base case in Fig. 10, it can be clearly found that the reduction of energy consumption for jet fuel regardless of the increase in total energy consumption. Moreover, it is found that the recycle system (90 % recycle) requires the lowest energy consumption for jet fuel (4.57 MW/t jet fuel) than other  $\rm CO_2$ -FTS processes and achieves the highest  $\rm CO_2$  conversion (85.8 %). This superior performance is attributed to the 90 % tail gas recycle, which produces the highest jet fuel yield.

# 5. Economic analysis of the modified CO<sub>2</sub>-FTS process for jet fuel production at commercial scale

#### 5.1. Economic methodology

The economic analysis of the  $CO_2$ -FTS process was conducted using the Aspen Process Economic Analyzer® (APEA) and the detailed process

table 10 Equipment installed cost breakdown for base case, multi-stage CO<sub>2</sub>-FTS and CO<sub>2</sub>-FTS with tail gas recycl

	Base case	Multi-stage CO <sub>2</sub> -FTS		CO <sub>2</sub> -FTS with tail gas recycle		
		Two-stage	Three-stage	63.8 % recycle	80.3 % recycle	90 % recycle
Equipment	Equipment installed cost (M\$) Equipment installed cost (M\$)	Equipment installed cost (M\$)	Equipment installed cost (M\$)	Equipment installed cost (M\$)	Equipment installed cost (M\$) Equipment installed cost (M\$) Equipment installed cost (M\$) Equipment installed cost (M\$)	Equipment installed cost (M\$)
$H_2$	57.61	57.61	57.61	57.61	57.61	57.61
compressor						
$CO_2$	13.14	13.14	13.14	13.14	13.14	13.14
compressor						
Heater	1.87	3.52	4.54	2.92		3.47
$CO_2$ -FTS	55.25	93.33	119.11	82.72	95.49	104.55
reactor						
Cooler	0.23	0.41	0.56	0.29	0.31	0.32
Three-phase	0.17	0.31	0.43	0.18	0.19	0.19
separator						

flowsheets are shown in Figs. 5–7. APEA calculates the purchased and installed equipment cost for CO<sub>2</sub>-FTS process such as the compressors, heater, cooler, from which the total direct cost of the plant is calculated. CAPEX is derived from the total direct cost with the accounting of other financial items such as indirect cost, engineering and contingency. The OPEX consists of the fixed operating and maintenance costs (fixed OPEX) and the variable operating and maintenance costs (variable OPEX). The fixed OPEX assumed as 3 % of CAPEX is made up of the total maintenance cost, labour costs, administration cost, and other cost [34]. The variable OPEX is based on feedstock cost and utility cost obtained from the APEA with their unit price.

The financial parameters used in the economic evaluation are shown in Table 9.  $CO_2$  is assumed to be free from a  $CO_2$  capture plant [35]. The hydrogen price was assumed to be \$2/kg which is the 2025 target of renewable hydrogen from electrolysis [36]. Other parameters are commonly used for the economic evaluation of a commercial plant [25,34,37].

It is noted that the  $CO_2$ -FTS reactor cannot be mapped in APEA, therefore it was considered as zero cost. Alternatively, Eqs. (17) and (18) are used to calculate the equipment installed cost of the  $CO_2$ -FTS reactor, using an installation factor of 2.75 and a scaling exponent of 0.8. The base cost and base size are referred to Zang et al. [24].

Equipment installed cost = Purchased equipment  $cost \times Installation$  factor

(17)

Purchased equipment cost = Base cost 
$$\times \left(\frac{New \ size}{Base \ size}\right)^{Scaling \ exponent}$$
 (18)

The annual capital cost (ACC) was calculated by annualizing the CAPEX using Eq. (19) with plant lifetime n, and interest rate i.

$$ACC = CAPEX\left(\frac{i(1+i)^n}{(1+i)^n - 1}\right)$$

$$\tag{19}$$

The total annual cost shown in Eq. (20) is the sum of ACC and OPEX.

Total annual 
$$cost = ACC + Fixed OPEX + Variable OPEX$$
 (20)

The MSP of jet fuel was obtained from the Eq. (21) [38].

$$MSP = \frac{Total \ annual \ cost}{Operating \ time \ per \ year \times Y_{Jetfuel}}$$
 (21)

#### 5.2. Economic evaluation results

The economic performance of the CO<sub>2</sub>-FTS process was performed for base case, multi-stage CO<sub>2</sub>-FTS, and CO<sub>2</sub>-FTS with tail gas recycle process. The installed equipment costs in Table 10 were obtained from APEA. It is noticeable that compressors and CO<sub>2</sub>-FTS reactors dominate the total equipment installed cost for different CO<sub>2</sub>-FTS processes. The installed cost of the CO<sub>2</sub> compressor and H<sub>2</sub> compressor remain constant at 13.1 M\$ and 57.6 M\$ for all CO2-FTS processes because the feedstock is only compressed initially and there is no pressure drop after gas compression. While the increase in equipment installed cost of the CO2-FTS reactor can be seen for both water removal configurations. With the addition of more stages, the installed cost of the CO2-FTS reactor is 93.3 M\$ for two stages process and 119.1 M\$ for three stages process. The increase in these costs is due to the addition of more reactors in the multi-stage process. For the tail gas recycle process, as the recycle ratio changes from 0 to 90 %, the installed cost of the CO<sub>2</sub>-FTS reactor varies from 55.3 M\$ to 104.6 M\$ due to the larger reactor size required.

Table 11 presents the CAPEX breakdown and Table 12 summarises the economic performance. The best economic performance for jet fuel production is achieved by CO<sub>2</sub>-FTS with 90 % tail gas recycle. This process can potentially reduce the MSP from \$5.87/kg to \$2.6/kg, which is only 44 % of the base case price. For comparison with current market

Table 11 CAPEX breakdown for base case, multi-stage  $CO_2$ -FTS and  $CO_2$ -FTS with tail gas recycle.

Paramet	er	Calculation method	Base case	Multi-stag	e CO <sub>2</sub> -FTS	CO <sub>2</sub> -FTS with tail gas recycle		
				Two- stage	Three- stage	63.8 % recycle	80.3 % recycle	90 % recycle
TDC	Total direct cost (M\$)		128.27	168.33	195.38	156.85	170.11	179.28
TIC	Total indirect cost	20 % of TDC	25.65	33.67	39.08	31.37	34.02	35.86
BEC	Bare erected cost	TDC + TIC	153.93	202.00	234.46	188.22	204.13	215.14
EC	Engineering and contactor	27 % of BEC	41.56	54.54	63.30	50.82	55.12	58.09
EPC	Engineering procurement and construction	127 % of BEC	195.49	256.53	297.77	239.04	259.25	273.23
PC	Process contingency	25 % of BEC	38.48	50.50	58.62	47.06	51.03	53.79
PJC	Project contingency	20 % of EPC + 5 % of BEC	46.79	61.41	71.28	57.22	62.06	65.40
TPC	Total plant cost	120 % of EPC $+$ 30 % of BEC	280.77	368.44	427.66	343.32	372.34	392.42
OC	Owner's cost	15 % of TPC	42.11	55.27	64.15	51.50	55.85	58.86
CAPEX	Total capital expenditure	115 % of TPC	322.88	423.71	491.81	394.82	428.19	451.28

Table 12 Summary of the economic evaluation of base case, multi-stage  $CO_2$ -FTS and  $CO_2$ -FTS with tail gas recycle.

Description			Base case	Multi-stage CO <sub>2</sub> -FTS		CO <sub>2</sub> -FTS with tail gas recycle		
				Two-stage	Three-stage	63.8 % recycle	80.3 % recycle	90 % recycle
CAPEX (M\$)			322.88	423.71	491.81	394.82	428.19	451.28
ACC (M\$/yr)			37.93	49.77	57.77	46.37	50.30	53.01
Fixed OPEX (M\$/yr)			9.69	12.71	14.75	11.84	12.85	13.54
Variable OPEX (M\$/yr)	Utility cost	Electricity	16.38	16.38	16.38	16.38	16.38	16.38
		Cooling water	0.61	0.91	1.09	0.93	1.07	1.18
		Heating	2.92	4.70	5.76	4.47	5.46	5.69
	Feedstock cost	$CO_2$	0.00	0.00	0.00	0.00	0.00	0.00
		$H_2$	241.92	241.92	241.92	241.92	241.92	241.92
Total annual cost (M\$/yr)			309.44	326.39	337.67	321.92	327.97	331.71
Minimum selling price of jet fuel (\$/kg) 5.87			5.87	3.69	3.05	3.55	2.97	2.60

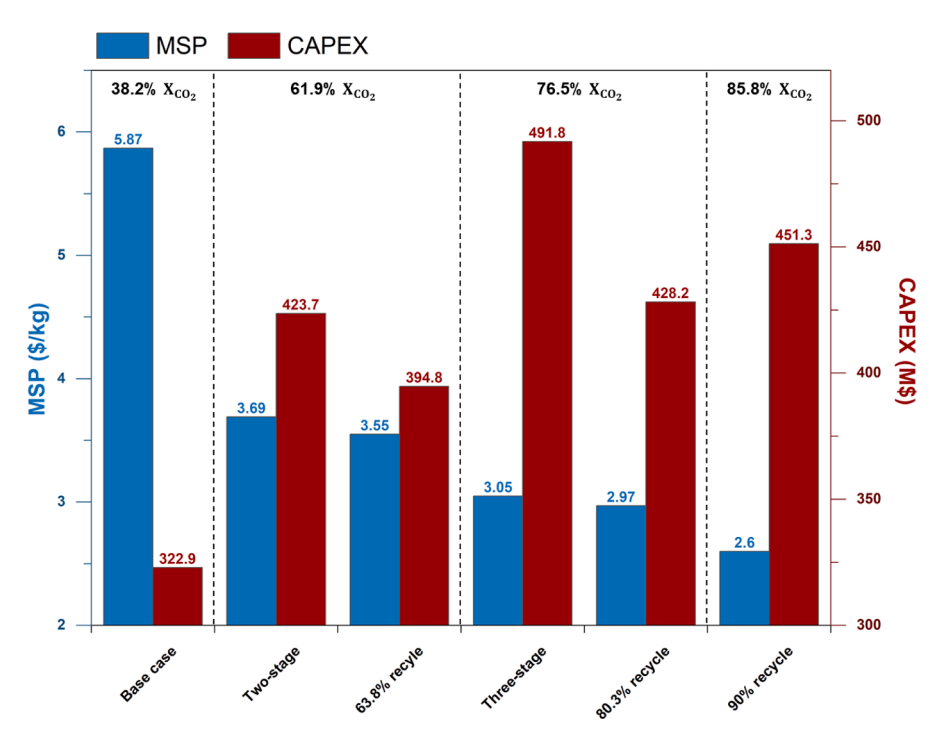


Fig. 11. Summary of MSP and CAPEX for different CO<sub>2</sub>-FTS process.

in 2022 [39], this is 2.4 times higher than the average market price of conventional jet fuel (\$1.1/kg), while it is only slightly higher than the SAF price in 2022 (\$2.4/kg). The three-stage  $\rm CO_2$ -FTS process was found to have the worst economic performance in terms of CAPEX and total annual cost. It is worth noting that the feedstock cost of hydrogen is the largest contributor to the total annual cost and MSP. For the base case

process, 78 % of the total annual cost comes from hydrogen costs. This is consistent with the previous study for the production of fuel based on  $CO_2$  and hydrogen [24]. Therefore, for reducing the MSP of jet fuel, the main goal is to investigate how to reduce the price of hydrogen.

#### 5.3. Comparison between two ex-situ water removal configurations

Two ex-situ water removal configurations were compared at the same CO2 conversion level (61.9 % and 76.5 %) for total cost and produced fuel cost. To clearly indicate the total cost for different process, the CAPEX was used for comparison instead of total annual cost. This is because the hydrogen demand is same for different process while hydrogen cost accounts roughly three quarters of total annual cost (Table 12). The economic analysis results shown in Fig. 11 indicate that the tail gas recycle process has lower CAPEX and MSP of jet fuel compared to the multi-stage process at the same CO2 conversion. For 61.9 % CO2 conversion case, the CAPEX is reduced from 423.7 to 394.8 M\$, and the MSP is reduced from 3.69 to 3.55 \$/kg. For 76.5 % CO<sub>2</sub> conversion, these values are from 491.8 to 428.2 for CAPEX and from 3.05 to 2.97 for MSP. Surprisingly, the CAPEX for the 90 % tail gas recycling process is 451.3 M\$, which is even lower than 491.8 M\$ for the three-stage process. This means that the 90 % tail gas recycling process can achieve higher CO2 conversion (85.8 %), but with lower invested CAPEX. From an economic point of view, the CO<sub>2</sub>-FTS process with tail gas recycle can save costs compared to the multi-stage CO<sub>2</sub>-FTS process.

#### 6. Conclusion

In this study, a CO<sub>2</sub>-FTS model for jet fuel production was developed in Aspen Plus® linked to ACM. The model was validated at the lab scale using experimental ASF plots and hydrocarbon selectivity. Technical analysis was conducted to predict the performance improvement of the commercial CO2-FTS process through two ex-situ water removal configurations. Compared to the base case scenario, the three-stage CO<sub>2</sub>-FTS process achieved a doubling (100 % increase) in both CO2 conversion and jet fuel yield. In the CO<sub>2</sub>-FTS process with a 90 % tail gas recycle, CO<sub>2</sub> conversion and jet fuel yield increased by 124 % and 107 %, respectively. Although the highest total energy demand was identified for CO<sub>2</sub>-FTS with 90 % tail gas recycle (260 MW), this system has the lowest unit energy demand (4.57 MWh per ton of jet fuel) due to the highest jet fuel productivity. For the same level of CO2 conversion, the multi-stage CO<sub>2</sub>-FTS behaves almost identically to the CO<sub>2</sub>-FTS with tail gas recycle. Further indications from the economic analysis show that the tail gas recycle has lower CAPEX and MSP costs due to the use of less equipment compared to the multi-stage CO<sub>2</sub>-FTS process. In conclusion, CO<sub>2</sub>-FTS with a high tail gas recycle rate has the potential to improve the performance of commercial CO2 utilisation plants from both technical and economic point of views.

#### CRediT authorship contribution statement

Yide Han: Writing – original draft, Validation, Software, Methodology, Formal analysis, Conceptualization. Ariane D.N. Kamkeng: Writing – review & editing, Validation, Software, Methodology. Olajide Otitoju: Writing – review & editing. Yuxing Ding: Writing – review & editing. Meihong Wang: Writing – review & editing, Supervision.

#### Declaration of competing interest

The authors declare that they have no known competing financial interests or personal relationships that could have appeared to influence the work reported in this paper.

#### Acknowledgements

The authors would like to acknowledge the financial support of the EU RISE project OPTIMAL (Grant Agreement No: 101007963).

# Data availability

Data will be made available on request.

#### References

- [1] Pörtner H-O, Roberts DC, Tignor M, Poloczanska ES, Mintenbeck K, Alegría A, et al. Climate Change 2022: Impacts, Adaptation and Vulnerability. Contribution of Working Group II to the Sixth Assessment Report of the Intergovernmental Panel on Climate Change Cambridge University Press, Cambridge, UK and New York, NY, USA; 2022.
- [2] IEA. Net Zero by 2050; 2021. Available from: https://www.iea.org/reports/net-zero-by-2050. [Accessed November 6, 2023].
- [3] Bergero C, Gosnell G, Gielen D, Kang S, Bazilian M, Davis SJ. Pathways to net-zero emissions from aviation. Nat Sustainability 2023;6(4):404–14.
- [4] IEA. Aviation; 2022. Available from: https://www.iea.org/energy-system/transport/aviation. [Accessed November 6, 2023].
- [5] THUNDER SAID ENERGY. Jet fuel demand: by region and forecasts to 2050?; 2023. Available from: https://thundersaidenergy.com/downloads/global-jet-fuel-demand-by-region-and-forecasts/. [Accessed November 6 2023].
- [6] Vardon DR, Sherbacow BJ, Guan K, Heyne JS, Abdullah Z. Realizing, "net-zero-carbon" sustainable aviation fuel. Joule 2022;6(1):16–21.
- [7] IEA. Putting CO<sub>2</sub> to Use; 2019. Available from: https://www.iea.org/reports/ putting-co2-to-use. [Accessed October 20, 2023].
- [8] Ishaq H, Crawford C. CO<sub>2</sub>-based alternative fuel production to support development of CO<sub>2</sub> capture, utilization and storage. Fuel 2023;331:125684.
- [9] Zang G, Sun P, Yoo E, Elgowainy A, Bafana A, Lee U, et al. Synthetic methanol/ Fischer-Tropsch fuel production capacity, cost, and carbon intensity utilizing CO<sub>2</sub> from industrial and power plants in the United States. Environ Sci Tech 2021;55 (11):7595–604.
- [10] van der Giesen C, Kleijn R, Kramer GJ. Energy and climate impacts of producing synthetic hydrocarbon fuels from CO<sub>2</sub>. Environ Sci Tech 2014;48(12):7111–21.
- [11] Zhou Z, Sun Z, Duan L. Chemical looping: A flexible platform technology for CH<sub>4</sub> conversion coupled with CO<sub>2</sub> utilization. Curr Opin Green Sustainable Chem 2022; 100721.
- [12] Dutta A, Farooq S, Karimi IA, Khan SA. Assessing the potential of CO<sub>2</sub> utilization with an integrated framework for producing power and chemicals. Journal of CO<sub>2</sub> Utilization 2017;19:49–57.
- [13] Li L, Liu Q, Huang T, Peng W. Mineralization and utilization of CO<sub>2</sub> in construction and demolition wastes recycling for building materials: A systematic review of recycled concrete aggregate and recycled hardened cement powder. Sep Purif Technol 2022:298:121512.
- [14] Desport L, Selosse S. An overview of CO<sub>2</sub> capture and utilization in energy models. Resour Conserv Recycl 2022;180:106150.
- [15] Bushuyev OS, De Luna P, Dinh CT, Tao L, Saur G, van de Lagemaat J, et al. What should we make with CO<sub>2</sub> and how can we make it? Joule 2018;2(5):825–32.
- [16] Kamkeng AD, Wang M. Technical analysis of the modified Fischer-Tropsch synthesis process for direct CO<sub>2</sub> conversion into gasoline fuel: Performance improvement via ex-situ water removal. Chem Eng J 2023;462:142048.
- [17] Ye R-P, Ding J, Gong W, Argyle MD, Zhong Q, Wang Y, et al. CO<sub>2</sub> hydrogenation to high-value products via heterogeneous catalysis. Nat Commun 2019;10(1):5698.
- [18] Zhang L, Dang Y, Zhou X, Gao P, van Bavel AP, Wang H, et al. Direct conversion of CO<sub>2</sub> to a jet fuel over CoFe alloy catalysts. The Innovation 2021;2(4):100170.
- [19] Choi YH, Jang YJ, Park H, Kim WY, Lee YH, Choi SH, et al. Carbon dioxide Fischer-Tropsch synthesis: A new path to carbon-neutral fuels. Appl Catal B 2017;202: 605–10.
- [20] Choi YH, Ra EC, Kim EH, Kim KY, Jang YJ, Kang KN, et al. Sodium-containing spinel zinc ferrite as a catalyst precursor for the selective synthesis of liquid hydrocarbon fuels. ChemSusChem 2017;10(23):4764–70.
- [21] Hwang S-M, Han SJ, Park H-G, Lee H, An K, Jun K-W, et al. Atomically alloyed Fe–Co catalyst derived from a N-coordinated Co single-atom structure for CO<sub>2</sub> hydrogenation. ACS Catal 2021;11(4):2267–78.
- [22] Yao B, Xiao T, Makgae OA, Jie X, Gonzalez-Cortes S, Guan S, et al. Transforming carbon dioxide into jet fuel using an organic combustion-synthesized Fe-Mn-K catalyst. Nat Commun 2020;11(1):6395.
- [23] Meiri N, Radus R, Herskowitz M. Simulation of novel process of  $CO_2$  conversion to liquid fuels. Journal of  $CO_2$  Utilization 2017;17:284–9.
- [24] Zang G, Sun P, Elgowainy AA, Bafana A, Wang M. Performance and cost analysis of liquid fuel production from H<sub>2</sub> and CO<sub>2</sub> based on the Fischer-Tropsch process. Journal of CO<sub>2</sub> Utilization 2021;46:101459.
- [25] Fernández-Torres MJ, Dednam W, Caballero JA. Economic and environmental assessment of directly converting CO<sub>2</sub> into a gasoline fuel. Energ Conver Manage 2022;252:115115.
- [26] Colelli L, Segneri V, Bassano C, Vilardi G. E-fuels, technical and economic analysis of the production of synthetic kerosene precursor as sustainable aviation fuel. Energ Conver Manage 2023;288:117165.
- [27] Atsonios K, Li J, Inglezakis VJ. Process analysis and comparative assessment of advanced thermochemical pathways for e-kerosene production. Energy 2023;278: 127868
- [28] Hillestad M. Modeling the Fischer-Tropsch product distribution and model implementation. Chem Prod Process Model 2015;10(3):147–59.
- [29] Donnelly TJ, Yates IC, Satterfield CN. Analysis and prediction of product distributions of the Fischer-Tropsch synthesis. Energy Fuel 1988;2(6):734–9.
- [30] Todic B, Bhatelia T, Froment GP, Ma W, Jacobs G, Davis BH, et al. Kinetic model of Fischer-Tropsch synthesis in a slurry reactor on Co–Re/Al<sub>2</sub>O<sub>3</sub> catalyst. Ind Eng Chem Res 2013;52(2):669–79.
- [31] Kallio P, Pásztor A, Akhtar MK, Jones PR. Renewable jet fuel. Curr Opin Biotechnol 2014;26:50–5.
- [32] Hemighaus G, Boval T, Bacha J, Barnes F, Franklin M, Gibbs L, et al. Aviation fuels technical review. Chevron Corporation 2006.

- [33] IATA. IATA guidance material for Sustainable Aviation Fuel Management. 2 ed.;
- Otitoju O, Oko E, Wang M. Technical and economic performance assessment of post-combustion carbon capture using piperazine for large scale natural gas combined cycle power plants through process simulation. Appl Energy 2021;292:
- [35] Shao B, Hu G, Alkebsi KA, Ye G, Lin X, Du W, et al. Heterojunction-redox catalysts of Fe<sub>x</sub>Co<sub>y</sub>Mg10 CaO for high-temperature CO<sub>2</sub> capture and in situ conversion in the context of green manufacturing. Energ Environ Sci 2021;14(4):2291-301.
- [36] ENERGY.GOV. Hydrogen production: Electrolysis; 2023. Available from: https:// www.energy.gov/eere/fuelcells/hydrogen-production-electrolysis#:~:
- text = Electrolysis%20 is%20 a%20 promising%20 option, a%20 unit%20 called%20 and all the statements of the statement of th
- %20electrolyzer. [Accessed 20 October 2023]. [37] Hepburn C, Adlen E, Beddington J, Carter EA, Fuss S, Mac Dowell N, et al. The technological and economic prospects for CO2 utilization and removal. Nature 2019;575(7781):87–97.
- [38] Martinez-Hernandez E, Ramírez-Verduzco LF, Amezcua-Allieri MA, Aburto J. Process simulation and techno-economic analysis of bio-jet fuel and green diesel production—Minimum selling prices. Chem Eng Res Des 2019;146:60-70.
- [39] IATA. IATA Economics; 2024. Available from: https://www.iata.org/en/ publications/economics/. [Accessed 20 August 2024].